Check for updates

Investigation on fluorescein derivatives with thermally activated delayed fluorescence and their applications in imaging†

Zhaoye Lv,[a] Jun Hou,[a] Junjie Yao,[a] Ye Yuan,[a] Yulan Qian,[a] Junyang Zhu,[a] Hongjuan Zhao,[a] Xiaoqing Xiong (ID) *[ab] and Chengqi Jiao*[c]

Fluorescein derivatives with thermally activated delayed fluorescence (TADF) show much stronger competition ability and vaster prospects than traditional fluorescein dyes due to their prominent long lifetime. It will be of great significance to synthesize more fluorescein derivatives with TADF. In this work, compounds **DCF-MPYA** and **FL** with TADF properties were obtained by fine tuning the substituents' structure on the basis of fluorescein derivative **DCF-MPYM**. Their long-lived triplet excited states (21.78 μs, 32.0 μs) were proved by nanosecond time-resolved transient difference absorption spectra. The steady-state and time-resolved fluorescence spectra showed that **DCF-MPYA** and **FL** exhibited red fluorescence around 645 nm and 651 nm, respectively. The results of sensitivity to oxygen and heavy atoms further demonstrated that the time-resolved fluorescence spectra originate from the delayed fluorescence. The time correlated single-photon counting (TCSPC) data indicated that **DCF-MPYA** and **FL** showed long-lived lifetimes of 13.16 μs and 23.72 μs, respectively. The energy gap (ΔE_{ST}) between the singlet (S_1) and triplet (T_1) states of **DCF-MPYA** and **FL** was calculated to be 3.32 meV and 9.98 meV from the decay rate of DF as a function of temperature. The small energy gap is conducive to the occurrence of efficient TADF at room temperature. Meanwhile, Gaussian calculation was employed to observe the electron density of **DCF-MPYA** and **FL** in the ground and excited states. The calculation results indicate that the shapes and energy levels of the highest occupied molecular orbitals (HOMOs), lowest unoccupied molecular orbitals (LUMOs), and LUMOs+1 for the monoanion and dianion forms are similar and thus **DCF-MPYA** and **FL** exhibit almost the same luminescence properties. Finally, **DCF-MPYA** and **FL** with low toxicity were used in confocal and time-resolved fluorescence imaging. Our construction strategy will be beneficial for developing more fluorescein derivatives with TADF in the future.

Introduction

Fluorescein dyes were first obtained from resorcinol and phthalic anhydride by von Bayer under the catalysis of zinc chloride in 1871. They have the advantages of large molar extinction coefficient,[1] high fluorescence quantum yield,[2] easy synthesis and purification,[3] and low environmental and biological toxicity.[4] Therefore, fluorescein is one of the fluorescent dyes which is widely used in the development of fluorescent

probes.[5] However, the traditional fluorescein dyes still have some disadvantages, such as: (1) the absorption and emission wavelengths for the designed fluorescent probes based on fluorescein dyes are mainly concentrated in the visible band, which limits the application of these fluorescent probes in the fields of clinical laboratory diagnosis and chemical biology;[6] (2) the fluorescein dyes have small Stokes shift (<25 nm), which causes fluorescence self-quenching and errors because of the Rayleigh scattering;[7] (3) the fluorescence lifetime (nanosecond scale) of fluorescein dyes is short, which brings about the interfere of background fluorescence.[8] Therefore, it is of great significance to develop fluorescein dyes with long emission wavelength, large Stokes shift and long-lived fluorescence lifetime.

In 1961, Parker and Hatchard discovered that eosin has the TADF property with long fluorescence lifetime.[9] Compared with traditional rare earth and transition metal complexes, eosin not only has long fluorescence lifetime but also has better biocompatibility. Thus, this excellent property has greatly attracted the scientific researchers' attention. Following the dye

[a]*Key Lab of Textile Cleaning, Dalian Polytechnic University, #1 Qinggongyuan, Dalian 116034, P. R. China. E-mail: xiongxq@dlpu.edu.cn; Fax: +86 41186323511; Tel: +86 41186332096*

[b]*State Key Laboratory of Fine Chemicals, Dalian University of Technology, 2 Linggong Road, Dalian 116024, P. R. China*

[c]*School of Chemistry and Chemical Engineering, Liaoning Normal University, 850 Huanghe Road, Dalian 116029, P. R. China. E-mail: jiaocq@lnnu.edu.cn*

eosin, Song group firstly introduced substituents at the position 4′ and 5′ of 2′, 7′-dichlorofluorescein (DCF) matrix through Duff and Knoevenagel reactions.[6] And they obtained the dye **DCF-MPYM** with long wavelength emission (λ_{em} > 590 nm), large Stokes shift (>150 nm) and long-lived TADF lifetime (22.11 μs in deoxy ethanol).[8] According to the characteristics of long-lived delayed fluorescence of **DCF-MPYM**, it was used in time-resolved fluorescence imaging to achieve the effect of no background fluorescent interference. Based on this derivation, this group has done a lot of application researches on the performance of TADF.[10–12] For example, **DCF-MPYM-N1** and **DCF-MPYM-N2** with the integration of nitro-reductase activated diagnosis and treatment were designed and synthesized on the basis of TADF fluorescein derivative **DCF-MPYM**.[10] They can be used for specific fluorescence diagnosis and photodynamic therapy of hypoxic tumours with overexpression of nitro-reductase. In 2018,[11] based on the fluorescence resonance energy transfer (FRET) mechanism, they developed the ratio hypochlorous acid fluorescent probe **FL-CyN** by utilizing **DCF-MPYM** as energy donor and cyanine as energy acceptor. In 2019,[12] they constructed dual targeted diagnosis and treatment integration photosensitizer **FL-RGD** through covalently coupling TADF fluorescein derivative **FL** with cyclic tripeptide RGD, which was successfully applied to the integration of tumour diagnosis and treatment. Therefore, the above results show that developing more fluorescein derivatives with TADF is significant for the future research of fluorescent diagnosis and photodynamic therapy.

It is assumed that it will be possible to obtain fluorescein derivatives with TADF property by fine tuning the substituents' structure on the basis of **DCF-MPYM**. In this study, 2,6-dimethyl-4H-pyran-4-ylidene malononitrile used for constructing **DCF-MPYM** was transformed to 2-cyano-2-(2,6-dimethyl-4h-pyran-4-ylidene) ethyl acetate, DCF derivative **DCF-MPYA** with long delayed fluorescence lifetime was synthesized (Scheme 1). Meanwhile, another fluorescein derivative **FL** was obtained by adjusting the ortho-carboxyl group on the benzene ring to the para-position. Their structures were characterized by ^{1}H, ^{13}C NMR and high-resolution mass spectrometry. The luminescence properties of **DCF-MPYA** and **FL** were analysed by the steady-state fluorescence spectroscopy, time-resolved fluorescence spectroscopy, nanosecond transient absorption technology and fluorescence lifetime. All the results indicated that both **DCF-MPYA** and **FL** showed long-lived lifetimes and TADF. Besides, the density functional theory (DFT) was used to observe the electron density

of **DCF-MPYA** and **FL** at the ground and excited state. The calculation results show that the shapes and energy levels of HOMOs, LUMOs, and LUMOs+1 for monoanion and dianion forms are similar. Thus, it explains the reason that **DCF-MPYA** and **FL** exhibit almost same luminescent properties through the analysis of electron density. The aforementioned results show that fine tuning the structures of dyes with TADF property is helpful to construct new TADF dyes. Our constructing strategy of fluorescent dyes and the research methods will be conducive to the development of more organic dyes with TADF in the future.

Materials and synthesis

Materials

Common reagents used in the experiments were all of analytical grade. Urotropine, trifluoroacetic acid, piperidine, 2-cyano-2-(2,6-dimethyl-4h-pyran-4-ylidene) ethyl acetate, and 2,6-dimethyl-4H-pyran-4-ylidene malononitrile are purchased from Aladdin. All the reactions were carried out under nitrogen (N_2) atmosphere with dry, freshly distilled solvents under anhydrous conditions, unless otherwise noted. Silica gel (100–200 mesh) was used for flash column chromatography.

Synthesis

Compound DCF-MPYA. To a solution of DCF dialdyhyde[6] (0.159 g, 0.348 mmol) in dry EtOH (50 mL)/CH$_3$OH (10 mL), ethyl 2-cyano-2-(2,6-dimethyl-4h-pyran-4-ylidene) ethyl acetate (0.147 g, 0.670 mmol) and piperidine (0.172 g, 2.00 mmol) were added under N_2 atmosphere. The mixture was refluxed for 24 h under N_2 atmosphere at 85 °C. After finishing reaction, the reaction mixture was allowed to cool to 25 °C, and then the solvent was evaporated in vacuum. After being purified by column chromatography on silica gel (elution : methanol/dichloroethane from 0.1 : 250 to 1 : 250), compound **DCF-MPYA** was obtained as black red powder (0.130 g, 0.152 mmol, 22.7% yield). R_f = 0.38 (5% CH$_3$OH in dichloromethane), ^{1}H NMR (400 MHz, CD_3OD) δ 8.23 (d, J = 6.7 Hz, 1H), 8.17–8.04 (m, 2H), 7.88 (d, J = 7.6 Hz, 1H), 7.81–7.68 (m, 4H), 7.68–7.54 (m, 1H), 7.46 (d, J = 7.9 Hz, 1H), 7.04 (s, 2H), 6.48 (dd, J = 21.2, 9.3 Hz, 2H), 4.32–4.15 (m, 2H), 4.11 (dd, J = 10.4, 7.1 Hz, 2H), 2.39 (d, J = 6.4 Hz, 3H), 2.27 (d, J = 7.1 Hz, 3H), 1.35 (td, J = 7.1, 2.0 Hz, 3H), 1.27 (td, J = 7.0, 3.1 Hz, 4H). ^{13}C NMR (100 MHz, CD_3OD) δ 177.77, 176.99, 169.11, 166.51, 165.86, 161.96, 158.97, 158.15, 137.23, 134.04, 133.43, 133.03, 132.09, 124.66, 122.27, 115.32, 114.99, 111.51, 110.74, 110.05, 64.15, 48.41, 26.48, 25.84, 17.59. MS (ESI + Tof) m/z found 857.1311 for M − 1, calculated 858.1400 for C$_{46}$H$_{32}$Cl$_2$N$_2$O$_{11}$.

Compound FL. The synthesis method of intermediate and **FL** were according to the reported method.[12]

Results and discussion

Photophysical properties and nanosecond time-resolved transient difference absorption spectra of DCF-MPYA and FL

Firstly, the UV-vis absorption and steady-state emission spectra of **DCF-MPYA** and **FL** were studied (Fig. S1 and S2†) and
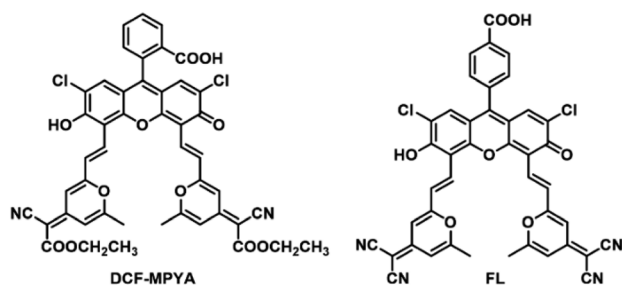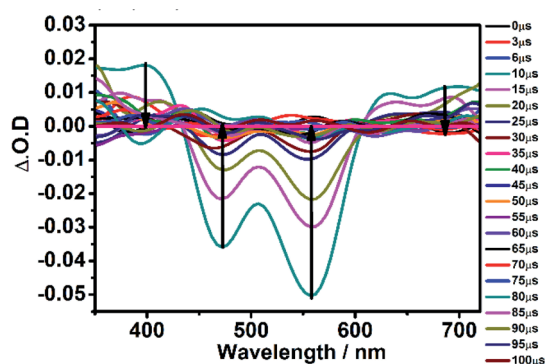

Scheme 1 The structures of DCF-MPYA and FL.

Fig. 1 Nanosecond time-resolved transient difference absorption spectra of **DCF-MPYA** (2.0×10^{-5} M in deaerated ethanol) with different delay time, excitation wavelength at 532 nm.
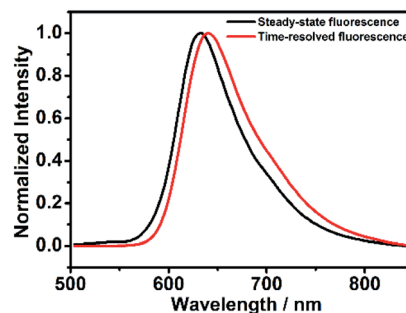

Fig. 2 Normalized emission spectra for **DCF-MPYA** (10.0 μM in deaerated CH_3CN). Black line: steady-state fluorescence spectrum under air atmosphere (delay time, 0 s). Red line: time-resolved fluorescence spectrum under N_2 atmosphere. All the delayed detection was carried out in phosphorescence mode (total decay time, 5 ms; delay time, 0.1 ms; gate time, 1.0 ms), and the excitation wavelength was 465 nm.

summarized in Tables S1 and S2.† **DCF-MPYA** and **FL** show two absorption peaks, both of them have large Stokes shifts (≥ 144 nm) in different organic solvents and exhibit slightly shorter in water (≤ 95 nm) (Tables S1 and S2†). However, the Stokes shifts of both dyes are much larger than those of conventional Rhodamine, Fluorescein and Rhodol dyes. Thus, it can be observed that the photophysical properties were similar with the reported compound **DCF-MPYM** in different solvents. Since the structures of **DCF-MPYA** and **FL** are analogous to **DCF-MPYM**, it is inferred that the luminescent characteristics of **DCF-MPYA** and **FL** may be consistent with those of **DCF-MPYM**. Thus, the spectra of two dyes will be studied in detail.

It was reported that the fluorescein derivative **DCF-MPYM** emits TADF and the most essential reason is the production of long-lived triplet state.[8] Therefore, it was expected that the **DCF-MPYA** and **FL** also can exhibit the same characteristic with **DCF-MPYM**. First, nanosecond time-resolved transient difference absorption spectra of **DCF-MPYA** and **FL** were carried out to prove whether the T_1 state of the fluorescein derivatives existed. As seen from Fig. 1, upon pulsed laser excitation at 532 nm, significant bleaching of the transient absorption bands was observed at about 400, 466, 561, and 650 nm in the range of 300–700 nm. The bleaching peaks at 466 nm and 561 nm were attributed to the depletion of the ground state of **DCF-MPYA**. Transient absorption bands at about 400 nm and 650 nm were due to the transient absorption of T_1 for **DCF-MPYA**. The T_1 lifetime for the transients of **DCF-MPYA** was determined as 21.78 μs in deaerated ethanol (Fig. S3A†). Similar transient spectra were also observed for **FL** in Fig. S4† and the T_1 lifetime of **FL** was estimated as 32.0 μs (Fig. S3B†). These results indicate that both the compounds **DCF-MPYA** and **FL** exhibit long-lived triplet excited state upon visible light excitation, therefore, the existence of long lifetime triplet state will provide prerequisite for the TADF property of **DCF-MPYA** and **FL**.

Luminescence spectra of DCF-MPYA and FL

Next, to investigate whether the luminescence spectra of **DCF-MPYA** and **FL** were related to the long-lived triplet lifetime, the steady-state and time-resolved fluorescence spectra were studied and recorded by using fluorescence spectrophotometer. As displayed in Fig. 2, a strong peak at 645 nm was observed in time-resolved fluorescence spectrum (delayed fluorescence, DF), which closely agreed with the prompt fluorescence (PF, 634 nm) in steady-state fluorescence spectrum at room temperature. It can be found that the delayed spectrum of **DCF-MPYA** showed a little red-shift in comparison with the steady-state fluorescence spectrum, and similar results were also observed on **FL** (Fig. S5†). The maximum steady-state and time-resolved emission wavelengths of **FL** peaked at about 649 nm and 651 nm, respectively. The red-shift phenomenon was observed in the previous report.[8] It can be attributed to the difference of nuclear configuration between the singlet and triplet excited states of **DCF-MPYA** and **FL**. According to the above results, it may be inferred that the prompt and delayed fluorescence spectra simultaneously contribute to the long wavelength region of **DCF-MPYA** and **FL**. Meanwhile, the time-resolved fluorescence spectra were relevant with their triplet state lifetimes.

As we all know, the triplet state is sensitive to oxygen[13] and heavy atom.[14] Thus, the time-resolved spectra will be affected by the deoxygenation and addition of substances containing heavy atoms. To clarify the origination from the delayed component, the time-resolved spectra of **DCF-MPYA** and **FL** were also measured with and without N_2 bubbling. It was found that the luminescence intensity of **DCF-MPYA** at 645 nm enhanced rapidly after deoxygenation (Fig. 3), and the measured photoluminescence intensity of **DCF-MPYA** in N_2 rich environment has 20 times enhancement than that in air atmosphere. Meanwhile, **FL** also shows the similar result, the luminescence intensity at 651 nm has 4 times enhancement after deoxygenation (Fig. S6†). In addition, the steady-state fluorescence spectra of **DCF-MPYA** and **FL** were also recorded after deoxygenation (Fig. S7†). It was observed that the steady-state fluorescence spectra had no significant changes whether in non-deaerated or deaerated atmosphere. Furthermore, the delayed fluorescence spectra were also obtained after the addition of ethyl iodide into the **DCF-MPYA** and **FL** nitrogen-saturated solution (Fig. 4 and S8†). As we expected, it was noted that the time-resolved fluorescence spectra showed much enhancement
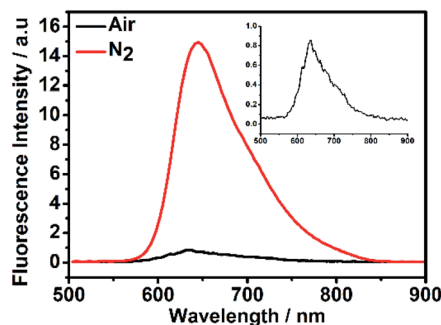
Fig. 3 Time-resolved fluorescence spectra for **DCF-MPYA** (10.0 μM in CH$_3$CN). Black line: time-resolved fluorescence spectrum under air atmosphere. Red line: time-resolved fluorescence spectrum under N$_2$ atmosphere. All the delayed detection was carried out in phosphorescence mode (total decay time, 5 ms; delay time, 0.1 ms; gate time, 1.0 ms), and the excitation wavelength was 465 nm.
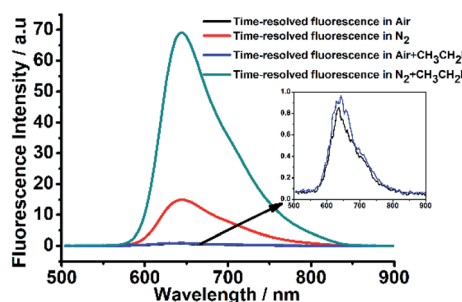

Fig. 4 Time-resolved fluorescence spectra for **DCF-MPYA** (10.0 μM in CH$_3$CN). Black line: time-resolved fluorescence spectrum under air atmosphere; red line: time-resolved fluorescence spectrum under N$_2$ atmosphere; blue line: time-resolved fluorescence spectrum after the addition of CH$_3$CH$_2$I under air atmosphere; dark cyan line: time-resolved fluorescence spectrum after the addition of CH$_3$CH$_2$I under N$_2$ atmosphere. Inset is the enlarged view of spectra with low fluorescence intensity. All the delayed detection was carried out in phosphorescence mode (total decay time, 5 ms; delay time, 0.1 ms; gate time, 1.0 ms), and the excitation wavelength was 465 nm.

at about 600–700 nm, but the steady-state fluorescence spectra exhibited no obvious enhancement (Fig. S7†). Thus, the above results further proved that the delayed emission at 645 nm and 651 nm results from the T$_1$ state of the derivatives and the time-resolved fluorescence can be attributed to TADF.

Luminescence lifetime measurement of DCF-MPYA and FL

It is known that the lifetime of delayed fluorescence can extend microsecond scale.[15–17] Here, the photoluminescent lifetime (PL) of **DCF-MPYA** and **FL** for nanosecond and microsecond time scale were measured by time correlated single-photon counting (TCSPC). As shown in Fig. S9–S12,† both the nanosecond and microsecond scale lifetimes of **DCF-MPYA** exhibit second-order exponential decay modal in N$_2$ atmosphere (Tables S3† and 1). The nanosecond scale lifetime of fast decay component at 634 nm was 4.20 ns in oxygen-free environment (Table S3†) and the delayed component decay of **DCF-MPYA**

Table 1 Fluorescent lifetime compositions of delayed components for **DCF-MPYA** and **FL** in deaerated CH$_3$CN. Excited at 485 nm (nanosecond pulsed OPO laser synchronized with spectrofluorometer) and monitored at 645 and 651 nm, respectively

Compound	$\tau_1{}^a$ (μs)	$n_1{}^b$ %	$\tau_2{}^a$ (μs)	$n_2{}^b$ %	$\tau_d{}^c$ (μs)
DCF-MPYA	0.92	40.73	21.58	59.27	13.16
FL	0.61	56.69	53.97	43.31	23.72

^{a} Obtained from the double-exponential fitting of transient decay curves on an 800 μs scale. ^{b} The contribution of each component to average lifetime. ^{c} The average fluorescence lifetime of delayed component.

after deoxynation complete within 13.16 μs (Table 1). After deaeration, the fluorescent lifetimes of **FL** for nanosecond and microsecond scale were 3.67 ns and 23.72 μs (Tables 1 and S4†), respectively. According to the results of lifetime, it can be concluded that the delayed lifetimes of **DCF-MPYA** and **FL** enhanced at least 1000 times in comparison with traditional fluorescent dyes. Thus, the long wavelength emission can be attributed to the spectral overlap of PF and DF. In other words, the DF at long wavelength region exhibits almost same spectrum as the PF based on the time-resolved and steady-state fluorescence.[18] Therefore, there is a fluorescence intensity ratio (I_{DF}/I_{PF}) between PF and DF. According to the reported calculation strategy,[8,19] the intensity ratio I_{DF}/I_{PF} of **DCF-MPYA** and **FL** can be approximately calculated to be 3.07 at 645 nm and 6.97 at 651 nm, respectively. This result suggests that the long wavelength region predominantly originates from the slow decay of long-lived DF component.

The energy difference estimation between S$_1$ and T$_1$ of DCF-MPYA and FL

Literature reported that the small energy difference between the S$_1$ and T$_1$ plays a significant role in the realization of reverse intersystem conversion (RISC) in pure organic fluorescent dyes.[8] It is the prerequisite to realize efficient TADF. The energy difference can be quantitatively calculated by the equation:

$$k_{ISC}^{T \to S} = \bar{k}_{ISC}^{T \to S} \exp(-\Delta E_{ST}/k_B T) \quad (1)$$

where k_B is Boltzmann's constant, T is temperature, and $\bar{k}_{ISC}^{T \to S}$ is the average rate constant for ISC. The lifetime of DF is mainly determined by RISC ($k_{ISC}^{T \to S}$) and thus the decay rate of DF can be used to represent $k_{ISC}^{T \to S}$ for ΔE_{ST} estimation. Here, the temperature-dependent long lifetimes for **DCF-MPYA** and **FL** were measured at 640 nm from 77 K to 300 K (Tables S5 and S6†). Then the logarithm of the fluorescence decay rate vs. the reciprocal of temperature for **DCF-MPYA** and **FL** was obtained in Fig. 5 and S13,† the red fitting curves were obtained on the basis of eqn (1). The energy gap between the S$_1$ and T$_1$ (ΔE_{ST}) was calculated to be 3.32 meV for **DCF-MPYA** and 9.98 meV for **FL**, respectively. The small energy gap is profitable for efficient TADF.[20] The results were consistent with our previously reported results of **DCF-MPYM**, which fully proves that the luminescence mechanism of **DCF-MPYA** and **FL** is the same as the reported **DCF-MPYM**.[8]
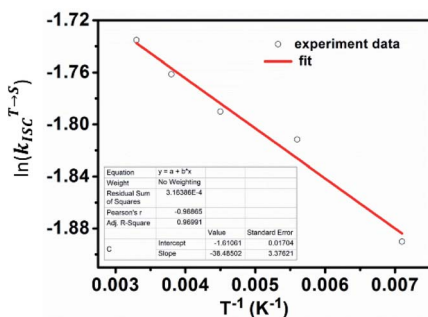
Fig. 5 Logarithm of the fluorescence decay rate *vs.* the reciprocal of temperature for **DCF-MPYA**; red line represents the fitting curves that obtained on the basis of eqn (1).

DFT calculations of DCF-MPYA and FL

To gain insight into the optical properties of **DCF-MPYA** and **FL**, their DFT calculations were performed using Gaussian 09 program. According to the reported literature,[21–23] the luminescence contribution of DCF derivatives may originate from the monoanion and dianion forms. Thus, the thermodynamically stable configurations for $[\text{DCF-MPYA-H}]^-$ (Fig. S14†), $[\text{DCF-MPYA-2H}]^{2-}$ (Fig. S15†), $[\text{FL-H}]^-$ (Fig. S16†), and $[\text{FL-2H}]^{2-}$ (Fig. S17†) were initially performed with empirical dispersion corrected PBE0 functional (D3BJ damping) and the 6-31G(d) basis set. The optimized conformation shows that the two appendant parts at the position of 4′ and 5′ exhibit a remarkable twist from xanthene moiety and appendant parts are parallel to each other. Meanwhile, the HOMO, LUMO, and LUMO+1 energy levels were calculated and presented in Fig. 6 and S18–S20.† At the ground and excited state, the electron densities on the HOMO, LUMO, and LUMO+1 of $[\text{DCF-MPYA-H}]^-$, $[\text{DCF-MPYA-2H}]^{2-}$, $[\text{FL-H}]^-$, and $[\text{FL-2H}]^{2-}$ distribute between appendant part, xanthene, and benzene ring moiety. All the electron density of HOMO for them mainly locates on the
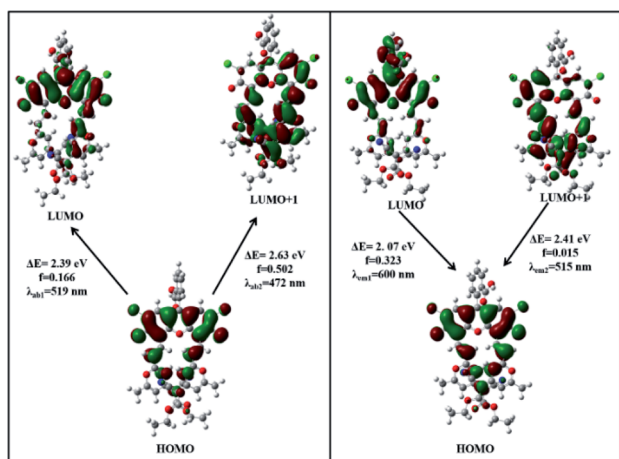
xanthene unit, the LUMO+1 electron density is positioned at the partial xanthene moiety as well as appendant part. The LUMO electron density for $[\text{DCF-MPYA-H}]^-$ and $[\text{FL-H}]^-$ mainly locates at xanthene unit and benzene ring, but electron density of LUMO for $[\text{DCF-MPYA-2H}]^{2-}$ and $[\text{FL-2H}]^{2-}$ distributes at xanthene unit and unilateral substituent. Despite the slightly structural difference between **DCF-MPYA** and **FL**, the shapes and energy levels of the HOMOs, LUMOs, and LUMOs+1 for monoanion and dianion forms are similar, which determines that the calculated absorption and emission wavelengths for **DCF-MPYA** and **FL** exhibit almost same (Tables S7–S10†). This also fully explains the reason that the two dyes actually have the same luminescence characteristics.

The confocal and time-resolved fluorescence imaging of DCF-MPYA and FL

Based on the excellent photophysical properties of **DCF-MPYA** and **FL**, they can be expanded to the biological application. First, low cytotoxicity of organic fluorophores is one of the important factors for live cells imaging.[24] MTT assays were performed in the MCF-7 cell lines by monitoring the absorbance of formazan at 570 nm to confirm the low cytotoxicity of **DCF-MPYA** and **FL**. As shown in Fig. 7, the low cytotoxicity of them *in vitro* was observed after different incubation time. Even the incubation time was extended to10 h, the cytotoxicity was moderately low for cells. Then the fluorescent images of **DCF-MPYA** and **FL** were performed on confocal fluorescence microscope. The results showed that both of them have good biocompatibility and they can well stain the MCF-7 cell lines (Fig. 8), thus they exhibit promising potential in biological application. To utilize the advantages of long-lived lifetime of **DCF-MPYA** and **FL**, the time-resolved fluorescence images of **DCF-MPYA** and **FL** were also taken from the laboratory-used time-domain luminescence microscope. As shown in Fig. 9, **DCF-MPYA** and **FL**-loaded MCF-7 cells emitted clearly red luminescence after 15 μs delay time. Thus, the aforementioned results manifested that **DCF-MPYA** and **FL** with TADF characteristic will be good candidates for fluorescent imaging.

Fig. 6 The frontier molecular orbital plots of $[\text{DCF-MPYA-H}]^-$ in DMSO; they are involved in vertical excitation (UV-vis absorption) and emission.
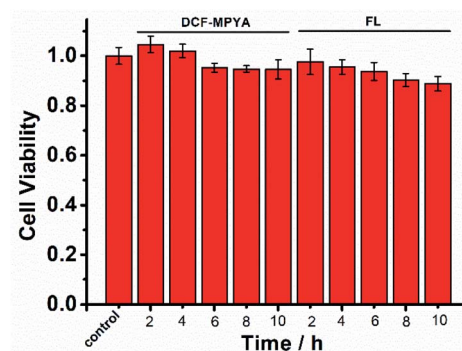

Fig. 7 Biological toxicity of MCF-7 cells in the presence of **DCF-MPYA** (20 μM), and **FL** (20 μM) was determined after different incubation time. Mean values and standard deviations are obtained from three independent experimental determinations.
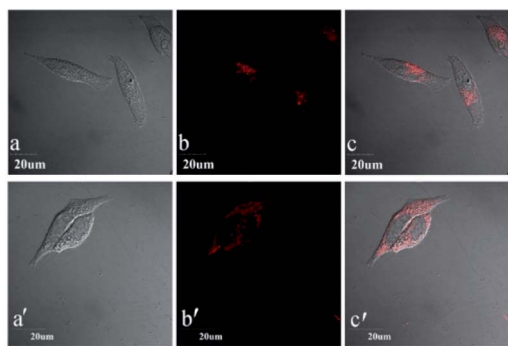
Fig. 8 Confocal fluorescence images of MCF-7 cells incubated with **DCF-MPYA** (20 μM), and **FL** (20 μM). (a) bright field image of cells for **DCF-MPYA**; (b) fluorescent image of cells for **DCF-MPYA** (λ_{ex} = 488 nm, λ_{em} = 580–620 nm); (c) the overlay of (a) and (b). (a') bright field image of cells for **FL**; (b') fluorescent image of cells for **FL** (λ_{ex} = 488 nm, λ_{em} = 580–620 nm); (c') the overlay of (a') and (b').
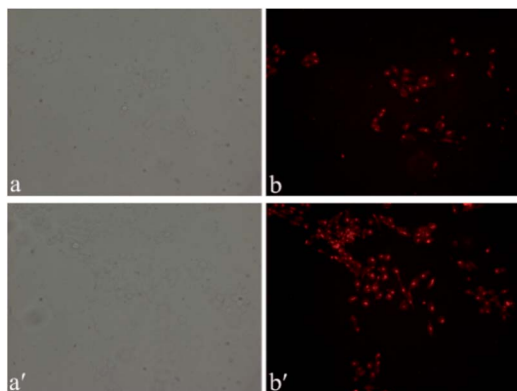

Fig. 9 (a) Bright-field luminescence images of MCF-7 after incubation with **DCF-MPYA** (20 μM); (a') Bright-field luminescence images of MCF-7 after incubation with **FL** (20 μM); (b) Time-gated luminescence images (excited with 510–560 nm) of MCF-7 after incubation with **DCF-MPYA** (20 μM); (b') Time-gated luminescence images (excited with 510–560 nm) of MCF-7 after incubation with **FL** (20 μM). The scale bars are 10 mm.

Conclusions

In summary, two red-emission fluorescein derivatives (**DCF-MPYA** and **FL**) with TADF property were synthesized on the basis of fine tuning the substituents' structure of **DCF-MPYM**. Luminescence characteristics of them were investigated by the nanosecond time-resolved transient difference absorption spectra, steady-state and time-resolved fluorescence spectra. The results indicated that **DCF-MPYA** and **FL** exhibited long-lived T_1 lifetime and delayed fluorescence. Then the lifetimes of delayed fluorescence for them were measured to be microsecond scale by TCSPC. Besides, the low energy gap between S_1 and T_1 was estimated to prove the reason for the occurrence of TADF. The DFT calculation results show that the shapes and energy levels of HOMOs, LUMOs, and LUMOs+1 for [**DCF-MPYA-H**]$^-$, [**DCF-MPYA-2H**]$^{2-}$, [**FL-H**]$^-$, and [**FL-2H**]$^{2-}$ are similar, which explains the reason that **DCF-MPYA** and **FL**

exhibit almost same luminescent properties. **DCF-MPYA** and **FL** were finally used in the confocal and time-resolved fluorescence imaging of MCF-7 cells, which proves that **DCF-MPYA** and **FL** will have great potentials in biological applications. This work manifests that fine tuning the structures of dyes with TADF property is helpful and provides a good platform for the development of more organic dyes with TADF in the future.

Author contributions

Z. Lv and X. Xiong contributed equally to this work. Zhaoye Lv: data curation, analytical measurements, original draft preparation and revision. Jun Hou: compounds' synthesis, data curation, original draft preparation. Junjie Yao: analytical measurements, data curation. Ye Yuan: analytical measurements, data curation. Yuanlan Qian: analytical measurements, data curation. Junyang Zhu: analytical measurements, data curation. Hongjuan Zhao: writing-reviewing. Xiaoqing Xiong: supervision and validation, methodology, conceptualization, writing-reviewing, and editing. Chengqi Jiao: DFT calculations.

Conflicts of interest

The authors declare no competing financial interest.

Acknowledgements

Notes and references

1 Y. Kushida, T. Nagano and K. Hanaoka, *Analyst*, 2015, **140**, 685–695.

2 X. F. Zhang, J. Zhang and L. Liu, *J. Fluoresc.*, 2014, **24**, 819–826.

3 A. Candreva, G. Di Maio and M. La Deda, *Soft Matter*, 2020, **16**, 10865–10868.

4 L. Huang, Y. Sun, G. Zhao, L. Wang, X. Meng, J. Zhou and H. Duan, *J. Mol. Struct.*, 2022, **1255**, 132427.

5 Y. Zhu, Y. Ma, Y. Liu, Z. Liu, S. Ma, M. Xing, D. Cao and W. Lin, *Sens. Actuators, B*, 2021, **327**, 128848.

6 X. Xiong, F. Song, S. Sun, J. Fan and X. Peng, *Asian J. Org. Chem.*, 2013, **2**, 145–149.

7 P. Shan, J. Yang, Z. Zang, Q. Zhao, Y. Cheng, L. Li, X. Yang, X. Yu, Z. Lu and X. Zhang, *Appl. Surf. Sci.*, 2021, **548**, 149287.

8 X. Xiong, F. Song, J. Wang, Y. Zhang, Y. Xue, L. Sun, N. Jiang, P. Gao, L. Tian and X. Peng, *J. Am. Chem. Soc.*, 2014, **136**, 9590–9597.

9 N. Li, F. Ni, X. Lv, Z. Huang, X. Cao and C. Yang, *Adv. Opt. Mater.*, 2022, **10**, 2101343.

10 Z. Liu, F. Song, W. Shi, G. Gurzadyan, H. Yin, B. Song, R. Liang and X. Peng, *ACS Appl. Mater. Interfaces*, 2019, **11**, 15426–15435.

11 Z. Liu, F. Song, B. Song, L. Jiao, J. An, J. Yuan and X. Peng, *Sens. Actuators, B*, 2018, **262**, 958–965.

12 Z. Liu, W. Shi, G. Hong, W. Chen, B. Song, X. Peng, X. Xiong and F. Song, *J. Controlled Release*, 2019, **310**, 1–10.

13 G. Zhang, G. M. Palmer, M. W. Dewhirst and C. L. Fraser, *Nat. Mater.*, 2009, **8**, 747–751.

14 Z. Huang, D. Ji, A. Xia, F. Koberling, M. Patting and R. Erdmann, *J. Am. Chem. Soc.*, 2005, **127**, 8064–8066.

15 R. Dong, J. Li, D. Liu, D. Li, Y. Mei, M. Ma and J. Jiang, *Adv. Opt. Mater.*, 2021, **9**, 2100970.

16 Y. Liu, L. Hua, Z. Zhao, S. Ying, Z. Ren and S. Yan, *Adv. Sci.*, 2021, **8**, 2101326.

17 S. Song, P. Zhang, H. Liu, X. Zhu, X. Feng, Z. Zhao and B. Z. Tang, *Dyes Pigments*, 2021, **196**, 109776.

18 T. Cardeynaels, S. Paredis, A. Danos, D. Vanderzande, A. P. Monkman, B. Champagne and W. Maes, *Dyes Pigments*, 2021, **186**, 109022.

19 X. Wen, P. Yu, Y.-R. Toh, A.-C. Hsu, Y.-C. Lee and J. Tang, *J. Phys. Chem. C*, 2012, **116**, 19032–19038.

20 M. K. Etherington, F. Franchello, J. Gibson, T. Northey, J. Santos, J. S. Ward, H. F. Higginbotham, P. Data, A. Kurowska and P. L. Dos Santos, *Nat. Commun.*, 2017, **8**, 1–11.

21 Y. Wu, Y. Zhao, P. Zhou, D. Zheng, H. Wang, S. Tang, J. Tian, S. Yang, W. Deng, K. Han and F. Song, *J. Phys. Chem. Lett.*, 2020, **11**, 5692–5698.

22 Y. Zhao, Y. Wu, W. Chen, R. Zhang, G. Hong, J. Tian, H. Wang, D. Zheng, C. Wu and X. Jiang, *Adv. Opt. Mater.*, 2022, 2102275.

23 J. An, Y. Wu, M. Lu, K. Han, F. Song and X. Peng, *J. Photon. Energy*, 2018, **8**, 032103.

24 Y. Cheng, G. Li, Y. Liu, Y. Shi, G. Gao, D. Wu, J. Lan and J. You, *J. Am. Chem. Soc.*, 2016, **138**, 4730–4738.